Contactless Position Measurement of an Electrical Conductor using GMR Sensors

Deepak Ghavari and V. Kartik
Department of Mechanical Engineering
Indian Institute of Technology Bombay, Mumbai, India.
deepak.ghavari@iitb.ac.in, vkartik@iitb.ac.in.

2024 IEEE Sensors Applications Symposium (SAS) | 979-8-3503-6925-0/24/$31.00 ©2024 IEEE | DOI: 10.1109/SAS60918.2024.10636402

***Abstract*—This article introduces a new method for contactless position measurement of an electrical conductor (such as a current-carrying wire) using giant magneto-resistive (GMR) sensors. The readout circuit of this method is designed for high-range, high-sensitivity dynamic position measurement of proposed of thin stationary and moving wire. The developed method can be applied in precision applications such as diamond abrasive wire (DAW) sawing, wire electrical discharge machining (EDM), musical instruments and acoustics. The proposed method is based on the principle of electromagnetism, where a constant DC current is supplied to the wire to produce a magnetic field around it. This magnetic field varies non-linearly outside the wire in the radial direction; the non-linear field is sensed using a GMR sensor. The sensor's performance is evaluated in terms of characteristics such as linearity, sensitivity, resolution, and drift. The variation in the magnetic field strength affects such characteristics. The maximum signal-to-noise ratio (SNR) and, hence, the maximum sensitivity of 4.2 V/mm, and $\pm$ 3σ resolution of 10 μm are achieved in the operating range.**

***Index Terms*—Contactless position measurement, giant magneto resistive (GMR) sensor, sensor characterisation**

I. Introduction

Contactless position measurement of wire with high sensitivity and high resolution is a critical requirement in several high-precision applications such as diamond wire-sawing [1]–[3], wire EDM [4] and musical instruments and acoustics [5], [6]. Moreover, it is important to observe the dynamic behaviour of stationary and moving wires applications [1]. For example, diamond abrasive wire cutting machines are employed to slice silicon ingots into individual slices in the wafer and semiconductor manufacturing industry [7], and in solar cell manufacturing processes [8]. In the aerospace industry, they enable precise cutting of materials such as carbon fibre-reinforced composites without causing delamination [1].

Position measurement of small stationary and moving objects with high precision is challenging due to the size of the measured object ranging from micrometres to millimetres, which is the primary factor limiting the use of general purpose contact type low sensitivity position measurement sensors such as accelerometers [9], [10] and potentiometers [11]. Although several contactless wire position sensing schemes have been reported such as laser [12], ultrasonic [13], and vision based sensors [14], these sensors are designed for detecting large moving objects, primarily relying on incidence and reflection principles. They may therefore not perform well with small and thin moving objects due to factors that are not considered in their design, such as target visibility, alignment, and signal noise. However, for some contactless position measurement sensors such as capacitive [15], eddy current-based [16], interferometric [17] and inductive sensors [18] the bandwidth 10-20 kHz and resolution are limited. For a capacitive sensors, has been reported a resolution of 1 nm over a bandwidth of 100 kHz [19] and they can be used for contactless position measurement; however, the readout scheme is complex [20]. To effectively address the challenges in measuring the dynamic behaviour of stationary and moving wire, we have selected a GMR sensors, that enable by high sensitivity, high bandwidth, and low noise [21].

GMR sensors exhibit two times higher sensitivity than anisotropic magnetoresistance (AMR) sensors [22] and several orders of magnitude greater sensitivity than Hall effect sensors while enabling high resolution [23]. GMR sensors have proven to be a promising alternative to conventional sensors due to their advantages of a small form factor and simple readout schemes. Their suitability for high-bandwidth and nanoscale-resolution multiaxis closed-loop operation has been demonstrated for position sensing [24]. A key advantage of GMR sensors is their 1 MHz inherent bandwidth, very high sensitivity and high operating temperature range, from $-60\,^{\circ}$C to $125\,^{\circ}$C [25].

In this article, the development of a contactless position measurement system for wire using GMR sensors is presented. The sensor's working principle, magnetic field distribution and the sensing method are discussed. The noise distribution is measured at different sampling rates to statistically analyze the noise. From the distribution plots, a sampling rate was selected at which the standard deviation (σ) was minimum, and the output data followed the Gaussian distribution. Next that, the sensitive zone and the operating range of the sensor is determined to find the operating range of the sensor. The GMR sensing system is deployed in contactless position measurement of a wire experiment to benchmark its performance characteristics, such as linearity, sensitivity, resolution, noise, and drift.

II. Working Principle and Sensing Method

The fundamental principle of the proposed sensing method is based on the Biot Savart law, which describes the distribution of the magnetic field inside and outside a current-carrying conductor. This law states that the magnetic field at a point in space is the result of the contributions from all the infinitesimal current carrying elements along the conductor, as schematically depicted in Fig. 1(a). The strength of each contribution depends on the distance, orientation and magnitude of each current input as given in equation (1) [26]:

$$dB = \frac{\mu_0}{4\pi}\frac{Idl}{r^2}sin\theta \tag{1}$$

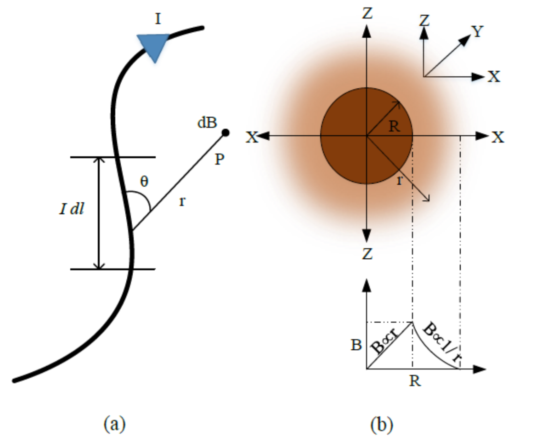

Fig. 1. (a) Schematic illustration of Biot Savart law and. (b) Schematic depiction of the magnetic field distribution inside and outside a circular conductor.

Where dB is the magnetic field due to a current element, μ_0 is the permeability of free space, I is the current flowing through the conductor, dl is an infinitesimal length element of the current-carrying conductor, and r is the distance from the conductor.

The magnetic field increases linearly with distance inside the wire and is proportional to the current's magnitude. Outside the wire, the intensity of the field decreases inversely as the distance from the wire's outer surface increases [27], as depicted in Fig. 1(b). This diminishing magnetic field strength is evident in the sensor's output voltage.

A known constant direct current (DC) is provided to the conductive wire via an external source, which generates a magnetic field around the wire. The produced magnetic field is sensed using the GMR sensor; such a sensor is highly sensitive to even very small changes in magnetic field strength. As compared to other conventional magnetic sensors, its operating principle is the phenomenon of giant magneto resistance, where the electrical resistance of the sensor's active material changes under the action of an externally-applied magnetic field. The GMR sensor-based position sensing method was first presented by Sahoo *et al.* [23] and is schematically depicted in Fig. 2.

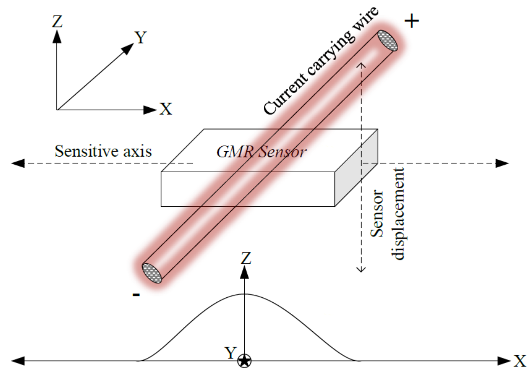

Fig. 2. Schematic depiction of the GMR sensing method.

We use a commercially-available GMR sensor (Model AA002-02, NVE Corporation, Eden Prairie, MN, USA). This sensor is set up as a Wheatstone bridge, with two active and two nickel-iron magnetic shielded elements-essentially a half-bridge, to compensate for temperature. It operates using both voltage and current excitation sources, but we have opted to use a voltage excitation drive source due to its simplicity and compatibility with many voltage excitation DAQ systems. The sensor's output voltage directly reflects the excitation amplitude from this bridge setup [25]. A GMR sensor's high sensitivity allows it to detect very small changes in magnetic field strength. The fundamental principle for position sensing is to convert a change in relative position into a corresponding change in magnetic field gradient, which is detectable by the GMR sensing elements. This is achieved by displacing the GMR sensor perpendicular to the wire surrounded by the magnetic field. This changes the magnetic field sensed by the GMR sensor; the corresponding change in sensor voltage is then read out as a position signal. After calibration, the conversion from position to voltage is given as follows:

$$\Delta V = \frac{dV}{dR}\frac{dR}{dB}\frac{dB}{dX}\Delta x + e_n \tag{2}$$

Where dB/dX is the change in the incident magnetic field with position, dR/dB is the corresponding change in the sensor's resistance, dV/dR is the change in the sensor's output voltage with a change in its resistance, and Δx is the position to be measured. e_n is an equivalent voltage noise source that accounts for the unavoidable noise in the measurement. While under ideal conditions, any infinitesimally small Δx should be detectable, e_n limits the achievable resolution, and the ratio of $\Delta V/e_n$ (SNR) becomes the resolution-limiting factor.

III. Statistical Analysis of Noise and Sensor Sensitivity

Before characterizing the sensor, statistical analysis of the output data was performed. In order to meet the requirements for statistical analysis, sensor output data should ideally follow a Gaussian distribution. This involves determining key metrics such as mean, standard deviation and root mean square (RMS), etc. [28], [29] of the error.

A fixed distance was maintained between the sensor and the current carrying wire to conduct this experiment. The magnetic field around the wire was sensed through the GMR sensor. The sensor's output voltage was acquired through a data acquisition (DAQ) device (Model Labjack U3-HV, W Jefferson Ave, Lakewood, USA) [30]. The experiment was conducted at sampling rates of 5 to 50 kHz in 5 kHz steps. Fig. 3 shows

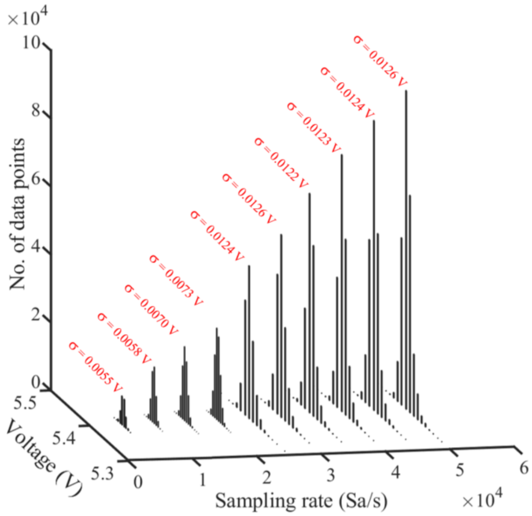

Fig. 3. Noise distribution at different sampling rates.

the noise distribution plot at the different sampling rates. It is seen that the distribution is largely normal across all sampling rates but has different standard deviations. Generally, for the actual machines containing vibrating wire, the frequency of the vibration does not go beyond 1-1.5 kHz (which is an even more conservative number selected here) [31]. Therefore, to meet the criteria of the Nyquist–Shannon sampling theorem and capture the actual vibratory signal, a sampling rate of 10 kHz has been selected, which is approximately ten times the actual wire vibration signal. Sampling higher than 10 kHz not only increases standard deviation but also unnecessarily increases the data processing load on hardware as well as software. Fig. 3 shows that at the selected 10 kHz sampling rate, the standard deviation is 0.0058 V which is closer to the minimum standard deviation, and hence, further sensor characterization this sampling rate is used.

The size of the GMR sensor integrated circuit (IC) is 5*4 mm (length*width), but the whole IC are not equally sensitive along its length. To confirm their sensitive zone the experiments were conducted along the longitudinal axis of the GMR sensor. In this experiment the sensor was moved parallel to a current carrying wire. The point where the voltage change exhibited the maximum slope relative to the longitudinal axis was identified. The outcome of this experiment helped to find the optimal working range, with superior sensor performance. Subsequently, all experiments were conducted at this identified position. Fig. 4 shows that the maximum voltage slope occurred at 2 ± 0.5 mm along the sensor's longitudinal axis. The sensor showed maximum sensitivity and sensed even a weak magnetic field intensity at this operating range.

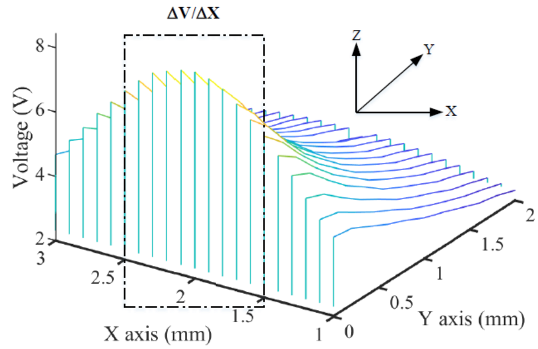

Fig. 4. Sensitivity zone of the GMR sensor.

IV. Experimental Analysis

In the experimental setup, a copper wire with a 0.25 mm diameter was used, and both ends of the wire were clamped to ensure adequate tension. A known DC current is supplied through the power supply to generate the magnetic field. The GMR sensor was employed to sense the produced magnetic field around the wire. The sensor's output voltage is very low; through this, it is challenging to detect the small positions. To overcome this limitation, we amplified the sensor's output using an instrumentation amplifier (Model INA 118P, Texas Instruments, Dallas, Texas, USA) with a 1k gain resistor, resulting in a gain of 51. This INA is known for its low drift, high common mode rejection ratio (CMRR), and low noise in the output signal [32]. The sensor was mounted on an XYZ positioning stage to displace the sensor. The experiment was conducted at the selected sampling rate, and the sensor's output voltage was recorded using the DAQ device; Fig. 5 illustrates the schematic of the circuit, while Fig. 6 depicts the experimental setup.

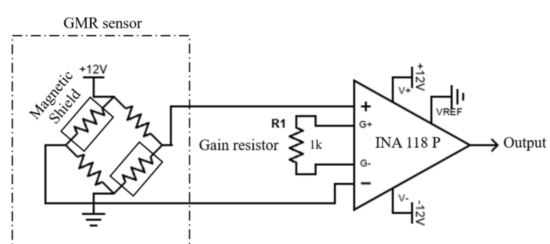

Fig. 5. Implemented GMR sensor readout circuit.

V. Sensor Characterization

In order to evaluate the performance of any position sensor, it is necessary to precisely define the characteristics of interest. Currently, terms such as linearity, sensitivity, resolution, noise,

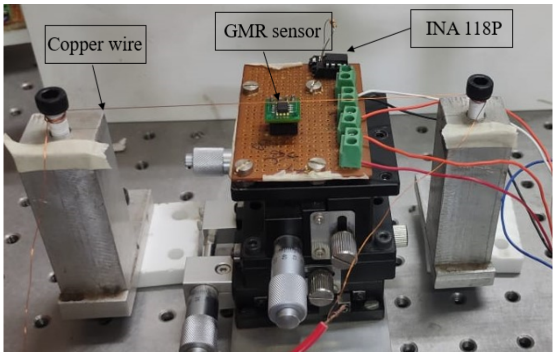

Fig. 6. Experimental setup for contactless position measurement of a wire using a GMR sensor.

and drift are loosely defined and often vary between manufacturers and researchers. The lack of a universal standard makes it difficult to predict the performance of a particular sensor from a set of specifications.

The magnetic field intensity inside a constant current-carrying wire exhibits a linear variation, ranging from zero at the center of the wire to a maximum at the periphery of the wire. The magnetic field is weak as one moves away in the radial direction of the wire, resulting in a high change in resistance in the GMR sensor's elements. Consequently, the rate of change in voltage per unit of position $\Delta V/\Delta x$ is high. As the distance from the wire increases, the change of slope $\Delta V/\Delta x$ change becomes small, leading to a logarithmic behavior in the output voltage of the GMR sensor relative to the input position, as depicted in Fig. 7.

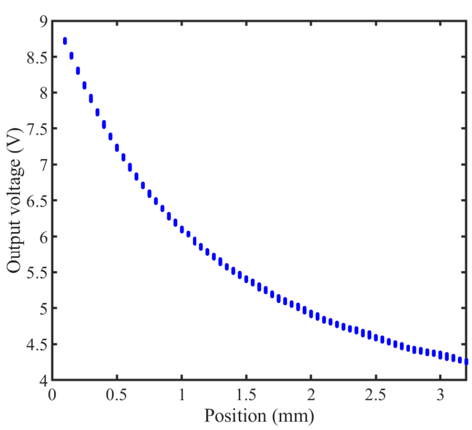

Fig. 7. Scatter plot of position vs output voltage.

For improving the sensor's accuracy and simplifying the calibration and interpolation process, it is desirable for the sensor's output voltage to change linearity relative to the input position. We see that the full-scale range of the developed sensor follows a logarithmic trend relative to the input position. However, specific sub-ranges reveal that the sensor's output voltage shows an approximate linear range within the 1.45 to 1.95 mm position. Within this linear range, the maximum voltage deviation is 15 mV, as shown in Fig. 8.

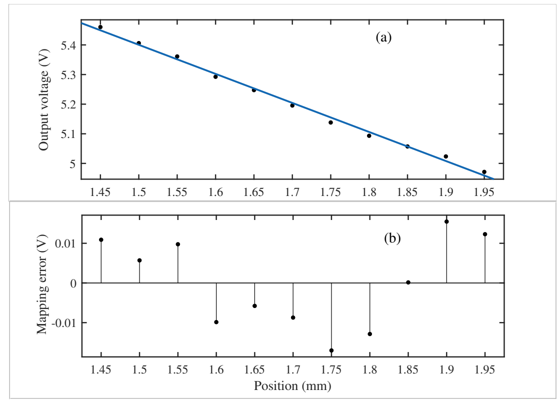

Fig. 8. (a) Linear voltage range of position vs output voltage. (b) Position vs mapping error.

Regression analysis was performed between the predicted position and the actual output voltage was fitted with a logarithmic function. The model equation for the predicted position was derived from such regression analysis between input position and output voltage. This equation provides the predicted position of the wire at the full-scale range. A plot of the predicted position against the actual position shows an approximate linear fit relative to the actual position. Fig. 9 shows that, except for some points, the deviation in the positions is less than 50 μm.

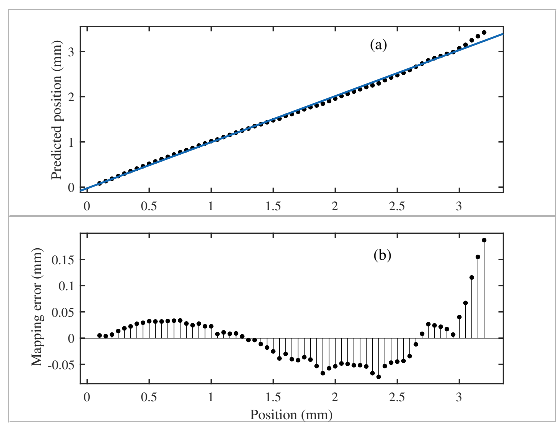

Fig. 9. (a) Linear fit of actual position vs predicted position. (b) Position vs mapping error.

Sensitivity plays a crucial role in the sensor's performance, as it determines the magnitude of change in output voltage for a corresponding change in the input position. Mathematically, sensitivity is defined by the slope of a curve $\Delta V/\Delta x$. Fig. 10 illustrates how sensitivity varies with input position. At the periphery of the wire, the intensity of the magnetic field is stronger, resulting in a higher voltage change per unit of position. However, as one moves away in the radial direction of the wire, due to weak magnetic field intensity the slope exhibits a decreasing trend. It diminishes the sensitivity and follows an approximate logarithmic pattern.

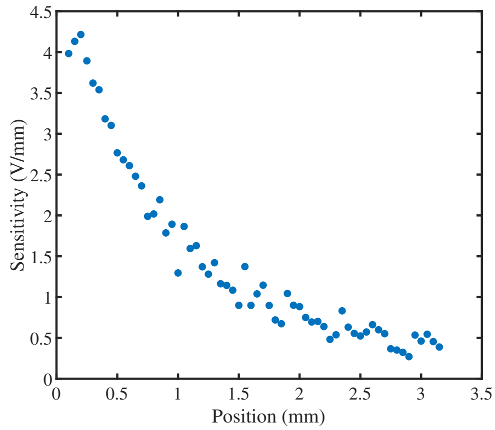

Fig. 10. Sensitivity variation across different positions.

Resolution is defined as the smallest detectable change that a sensor can measure. When noise follows a normal distribution, the resolution is expressed as $\pm\ 3\sigma$ [22]. Fig. 11 shows the variation in resolution with input position. Near the wire, where the magnetic field is more robust, signal strength is high, and 1/SNR is low, resulting in a low standard deviation. Conversely, moving away from the wire, where signal strength is low and 1/SNR is high, increases the standard deviation. Consequently, resolution is higher near the wire but decreases as one moves away.

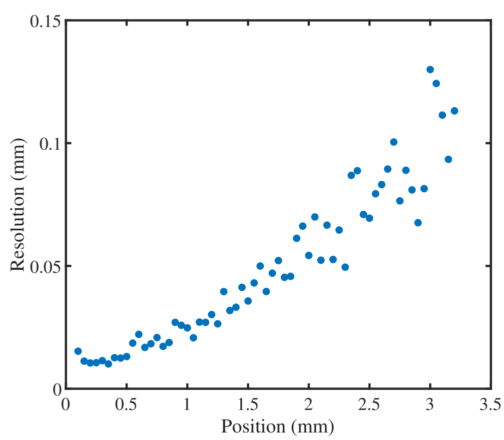

Fig. 11. Resolution variation across different positions.

Drift quantifies the extent to which the output voltage changes over a specified time duration under static conditions. Apart from intrinsic factors such as ohmic heating, it is primarily influenced by environmental factors such as temperature, humidity, vibration, dust, or gas composition. In proximity to the wire, at small distance, the high SNR results in minimal deviation of the output voltage. Conversely, moving away from the wire surface, the low SNR leads to higher deviation. As a result, drop "the depicted" Fig. 12 (a) shows a drift variation across different positions, and (b) shows a drift error at different positions. The larger gap between the maximum and minimum positions at 2.8 mm away from the wire surface. The maximum drift was 115 μm at a radial position of 3.05 mm.

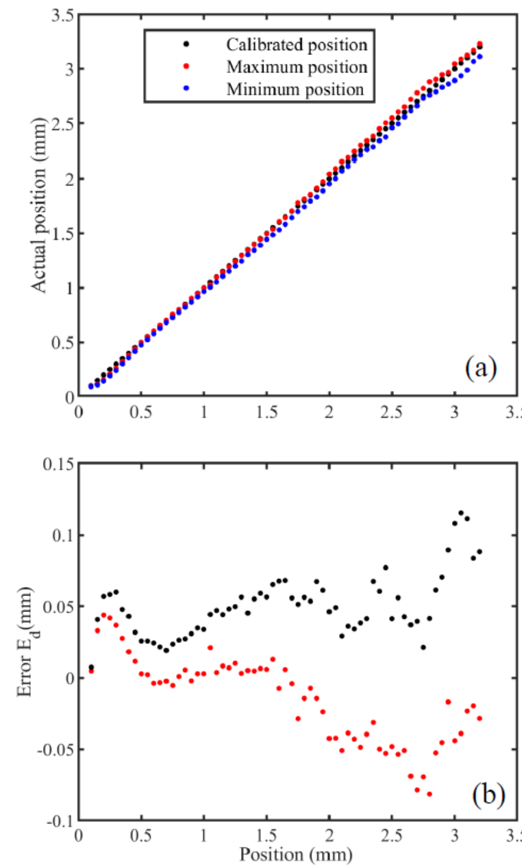

Fig. 12. (a) Drift variation across different positions. (b) Drift error at different positions.

VI. Summary

This article has introduced a novel method for contactless position measurement of wire using a GMR sensor; the readout circuit was designed for high range, high sensitivity. A known DC current was supplied through the external power source, and the magnetic field around the wire was generated. The intensity of this induced the magnetic field was sensed using the GMR sensor. The sensitivity is maximum close to the wire surface and exponentially decreases away from it. The maximum sensitivity is 4.2 V/mm, and the resolution was approximately 10 μm, which was not constant throughout the operating range. The observed linearity at a radial position of 1.45 mm from the wire surface was 0.5 mm. The maximum drift was 115 μm at a radial position of 3.05 mm.

References

[1] C. Zhang, Z. Dong, Y. Zhao, Z. Liu, S. Wu, and J. Yang, "Sawing force prediction model and experimental study on vibration-assisted diamond wire sawing," *Micromachines*, vol. 13, no. 11, p. 2026, 2022.

[2] K. Saptaji, S. Subbiah, and H. Zarepour, “A study of linear vibration-assisted scratching on silicon and its impact on the diamond wire wafering process,” in *28th European Photovoltaic Solar Energy Conference and Exhibition*, 2013.

[3] H. Huang, S. Wang, and X. Xu, “Effect of wire vibration on the materials loss in sapphire slicing with the fixed diamond wire,” *Materials Science in Semiconductor Processing*, vol. 71, pp. 93–101, 2017.

[4] S. Habib, “Optimization of machining parameters and wire vibration in wire electrical discharge machining process,” *Mechanics of Advanced Materials and Modern Processes*, vol. 3, pp. 1–9, 2017.

[5] C. Atteya and D. Campbell, *Giant Magnetoresistance Electric Guitar Pickup*. PhD thesis, Worcester Polytechnic Institute, 2016.

[6] A. U. Khan, D. K. Mandal, V. Visalakshi, B. George, and B. Bhikkaji, “A new tmr based sensing technique for electric guitar pickup,” in *2017 Eleventh International Conference on Sensing Technology (ICST)*, pp. 1–5, IEEE, 2017.

[7] L. Liang, S. Li, K. Lan, J. Wang, and R. Yu, “Fixed-diamond abrasive wire-saw cutting force modeling based on changes in contact arc lengths,” *Micromachines*, vol. 14, no. 6, p. 1275, 2023.

[8] T. Pu, Y. Gao, L. Wang, and Y. Yin, “Experimental investigation on the machining characteristics of fixed-free abrasive combined wire sawing pv polycrystalline silicon solar cell,” *The International Journal of Advanced Manufacturing Technology*, vol. 107, pp. 843–858, 2020.

[9] W.-m. Niu, F. Li-Qing, Z.-y. Qi, and D.-q. Guo, “Small displacement measuring system based on mems accelerometer,” *Mathematical Problems in Engineering*, vol. 2019, pp. 1–7, 2019.

[10] R. Dionisio, P. Torres, A. Ramalho, and R. Ferreira, “Magnetoresistive sensors and piezoresistive accelerometers for vibration measurements: A comparative study,” *Journal of Sensor and Actuator Networks*, vol. 10, no. 1, p. 22, 2021.

[11] K. Antonelli, J. Ko, and S. Ku, “Resistive displacement sensor,” *Measurement, Instrumentation, and Sensors Handbook: Two-Volume Set*, 2018.

[12] Y. S. Suh, “Laser sensors for displacement, distance and position,” 2019.

[13] M. Lian, H. Liu, T. Zhang, Q. Bo, T. Li, and Y. Wang, “Ultrasonic on-machine scanning for thickness measurement of thin-walled parts: Modeling and experiments,” *The International Journal of Advanced Manufacturing Technology*, vol. 104, pp. 2061–2072, 2019.

[14] D. Feng, M. Q. Feng, E. Ozer, and Y. Fukuda, “A vision-based sensor for noncontact structural displacement measurement,” *Sensors*, vol. 15, no. 7, pp. 16557–16575, 2015.

[15] S. Avramov-Zamurovic, N. G. Dagalakis, R. D. Lee, J. M. Yoo, Y. S. Kim, and S. H. Yang, “Embedded capacitive displacement sensor for nanopositioning applications,” *IEEE Transactions on Instrumentation and Measurement*, vol. 60, no. 7, pp. 2730–2737, 2011.

[16] V. Chaturvedi, J. G. Vogel, K. A. Makinwa, and S. Nihtianov, “A 19.8-mw eddy-current displacement sensor interface with sub-nanometer resolution,” *IEEE Journal of Solid-State Circuits*, vol. 53, no. 8, pp. 2273–2283, 2018.

[17] A. Miliou, “In-fiber interferometric-based sensors: Overview and recent advances. photonics, 8 (7), 265,” 2021.

[18] G. Chen, B. Zhang, P. Liu, and H. Ding, “An adaptive analog circuit for lvdt’s nanometer measurement without losing sensitivity and range,” *IEEE Sensors Journal*, vol. 15, no. 4, pp. 2248–2254, 2014.

[19] MicroSense, *MicroSense 6810 – High Resolution Capacitive Position Sensor,*, 2013. Microsense LLC, Lowell, MA, USA.

[20] B. George, Z. Tan, and S. Nihtianov, “Advances in capacitive, eddy current, and magnetic displacement sensors and corresponding interfaces,” *IEEE Transactions on Industrial Electronics*, vol. 64, no. 12, pp. 9595–9607, 2017.

[21] T. J. Joseph and V. Kartik, “Achieving low-noise, high-bandwidth, nanoscale-resolution position sensing with gmr sensors,” *IEEE Transactions on Instrumentation and Measurement*, 2023.

[22] A. J. Fleming, “A review of nanometer resolution position sensors: Operation and performance,” *Sensors and Actuators A: Physical*, vol. 190, pp. 106–126, 2013.

[23] D. R. Sahoo, A. Sebastian, W. Häberle, H. Pozidis, and E. Eleftheriou, “Scanning probe microscopy based on magnetoresistive sensing,” *Nanotechnology*, vol. 22, no. 14, p. 145501, 2011.

[24] V. Kartik, A. Sebastian, T. Tuma, A. Pantazi, H. Pozidis, and D. R. Sahoo, “High-bandwidth nanopositioner with magnetoresistance based position sensing,” *Mechatronics*, vol. 22, no. 3, pp. 295–301, 2012.

[25] NVE CORPORATION, *AA/AB-Series Analog Magnetic Sensors*, 2024. 11409 Valley View Road Eden Prairie, MN 55344-3617 USA.

[26] MIT, *Sources of Magnetic Fields*, 2020. 77 Massachusetts Avenue, Cambridge, MA, USA.

[27] MIT, *Sources of Magnetic Fields*, 2020. 77 Massachusetts Avenue, Cambridge, MA, USA.

[28] J. P. Stevens, *Intermediate Statistics: A Modern Approach*. Routledge, 2013.

[29] D. Wackerly, W. Mendenhall, and R. L. Scheaffer, *Mathematical Statistics with Applications*. Cengage Learning, 2014.

[30] LABJACK, *U3 DATASHEET*, 2020. LabJack Corporation 6900 West Jefferson Ave Suite 110 Lakewood, CO 80235 USA.

[31] A. Tang, Y. Fan, S. Li, and R. G. Landers, “Experimental and numerical studies of wire vibrations in bonded abrasive wire saw processing,” in *2016 International Symposium on Flexible Automation (ISFA)*, pp. 133–140, IEEE, 2016.

[32] TEXAS INSTRUMENTS, *INA118 Precision, Low-Power Instrumentation Amplifier*, 2020. DALLAS, USA.